

# Dramatic excitation dependence of strong and stable blue luminescence of ZnO hollow nanoparticles

Haibo Zeng,<sup>a)</sup> Shikuan Yang, Xiaoxia Xu, and Weiping Cai

Key Lab of Materials Physics, Anhui Key Lab of Nanomaterials and Nanotechnology, Institute of Solid State Physics, Chinese Academy of Sciences, Hefei 230031, People's Republic of China

(Received 30 September 2009; accepted 22 October 2009; published online 12 November 2009)

Strong and stable blue luminescence was obtained from ZnO hollow nanoparticles. Significantly, dramatic excitation dependence was observed for blue emissions of ZnO: (1) band-gap energy ( $E_g$ ) is the optimal excitation energy but smaller energies are still effective; (2) there exist several fixed emitting wavelengths in blue wave band, such as 412, 439, and 458 nm. These phenomena, combined with previously reported defect levels and formation thermodynamics, point out that the initial states of corresponding transitions to blue emissions could be zinc interstitials-related defect states, which were further verified by subsequent electron paramagnetic resonance examinations.

© 2009 American Institute of Physics. [doi:10.1063/1.3263712]

Wurtzite ZnO with exciton binding energy of 60 meV at room temperature (RT) has attracted researchers' attentions for several decades due to its many important applications in optical, electronic, optoelectronic, and piezoelectric devices.<sup>1,2</sup> Recently, the renewed impassioned interests in nanostructured ZnO are fueled and fanned by its attractive prospects on RT nanolaser, *p*-type doping, and RT ferromagnetic semiconductor,<sup>3,4</sup> etc. However, in spite of several decades of efforts, some of the basic natures of ZnO remain unclear, especially the identification of dominant intrinsic defects and defect origins of visible photoluminescence (PL).<sup>5,6</sup>

In the PL spectra of ZnO, typically there are emission bands in the UV<sup>7,8</sup> and visible (green, yellow, blue, and violet) regions. The UV emission is usually considered as the characteristic emission of ZnO and attributed to the band edge transition or the exciton combination.<sup>9</sup> Although the emissions in the visible regions are universally considered to be associated with the intrinsic or extrinsic defects in ZnO, there still exist extensive controversies for more than two decades on the clear defect centers and on the unambiguous electron transitions.<sup>10</sup> Compared with usually observed and intensively studied green emissions, blue luminescence of ZnO has been very unwanted, and its intensity and stability are very incompetent for the possible applications in light emitting and biological fluorescence labeling fields.<sup>11,12</sup> Most seriously, the corresponding origins are still unknown, blocking further understanding, controlling, and applications.

Herein, we report the intensive and stable blue PL from ZnO hollow nanoparticles (NPs) with special emphasis on its dramatic excitation dependence observed for the first time. These phenomena give out some important indications for the underlying defect origins with further verification from electron paramagnetic resonance (EPR).

The ZnO hollow NPs was fabricated by two steps of laser ablation in liquid (LAL) and subsequent acid etching as described previously.<sup>13,14</sup> The first step forms Zn/ZnO core/shell NPs, and the second hollows the NPs, preserving the ZnO nanoshells. The as-prepared powders were dried at 80 °C for 6 h, denoted as "sample A." The dry products

were further annealed at 200 °C for 6 h, denoted as "sample B." All the treatments were implemented in environmental atmosphere. The PL and PL excitation (PLE) spectra were measured using Xe lamp excitation (Edinburgh luminescence spectrometer FLS 920) with different excitation wavelengths at RT. The EPR measurement was conducted on an EPR-200 spectrometer using an X band (9.65 GHz).

The selected ZnO hollow NPs have average diameter of 20 nm and shell thickness of about 5 nm. There are many ultrafine nanocrystals and surrounding disordered areas inside the nanoshells.<sup>14</sup> Fig. 1(a) presents the comparison of the intensities of blue emissions from different samples. It is very clear that strong blue emissions can be obtained from ZnO hollow NPs after hollowing and drying (sample A) [curve 3 of Fig. 1(b)], whereas it is very weak in the primal Zn/ZnO NPs by LAL. After 200 °C annealing, such blue emissions are further enhanced more than ten times [sample

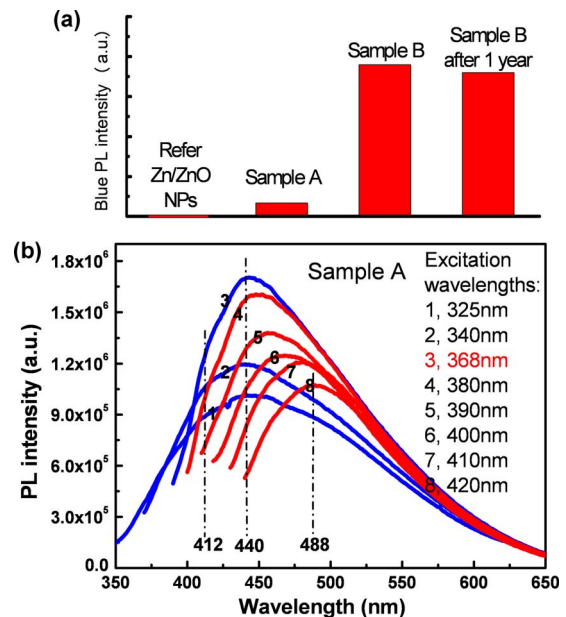


FIG. 1. (Color online) (a) Comparison of blue PL intensity from Zn/ZnO NPs, ZnO hollow NPs after 80 °C drying (sample A), ZnO hollow NPs after 200 °C annealing (sample B), and sample B after aging for one year; (b) ED-PL spectra of sample A.

<sup>a)</sup> Author to whom correspondence should be addressed. Electronic mail: hbzeng@issp.ac.cn.

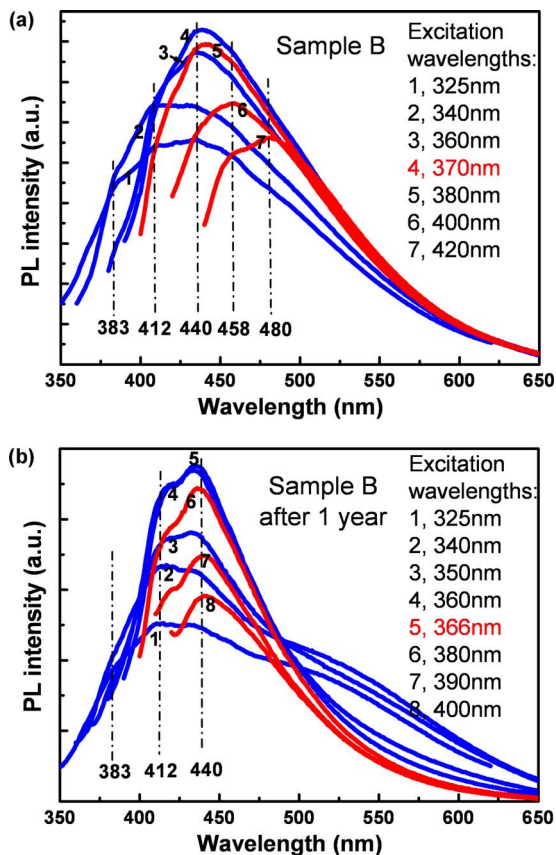


FIG. 2. (Color online) ED-PL spectra of sample B (a) and sample B after aging for one year (b).

B, curve 4 of Fig. 2(a)]. Furthermore, such strong blue emissions possess well stability with very slight weakening even after one year aging. These would break the intensity and stability blocks for future applications.

Figure 1(b) presents the excitation dependent PL (ED-PL) spectra of sample A. The evolution of blue emissions with excitation wavelengths can be separated into two regions. For curves 1, 2, and 3 in Fig. 1(b), the excitation energies are larger than band-gap energy ( $E_g$ ), which is assigned as 3.34 eV (corresponding to optimal excitation wavelength 368 nm and accordant with the PLE peak in Fig. 3). In this region, the emission intensity increases with excitation wavelength but the dominant peak at 440 nm and inconspicuous shoulder at 412 nm keep their positions changeless. For curves 4–8, the excitation energies become smaller

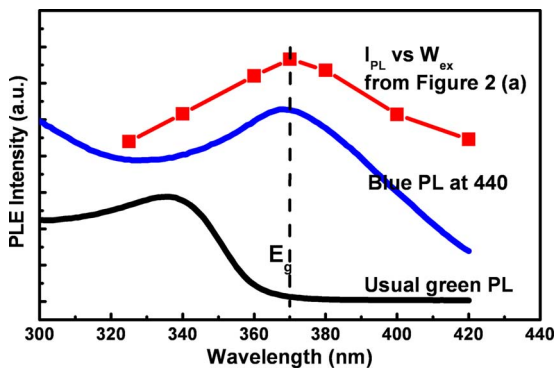


FIG. 3. (Color online) PLE spectra of present blue emission (439 nm) and usual green emission of ZnO.

than  $E_g$ . In this region, the emission intensity gradually decreases with further increase in excitation wavelengths but still preserves a high level and is comparable with the initial intensity, such as that of curve 1. The most remarkable difference is that the dominant peak positions redshift from 440 to 488 nm with the decrease in intensity.

Figure 2 presents the ED-PL spectra of sample B (annealed sample) and sample B after aging for one year. Under optimal excitation conditions, the dominant peak position at 440 nm [see curve 4 of Fig. 2(a)] is the same as sample A, whereas the intensity has been enhanced over ten times and then keeps almost invariable under long-term aging. Compared with sample A, the blue PL intensities also exhibit nonlinear increase-decrease dependence on excitation—first increase, reach saturation under  $E_g$  excitation, and then decrease but still effectively emit with excitation energy ( $E_{ex}$ ) smaller than  $E_g$ , as shown in Figs. 2(a) and 2(b). Among these universal excitation dependence features, the most important is that  $E_{ex}=E_g$  energy is the optimal excitation and  $E_{ex}<E_g$  energy can still effectively excite blue emissions.

The difference of ED-PL of sample A from B is also very clear and more significant. Replacing the redshift of dominant peak position for blue PL of sample B in Fig. 1(b), there emerge several very obviously fixed emitting wavelengths for blue PL of sample B: (1) 440 nm emitting point are observed in all curves as dominant peaks or shoulders; (2) 412 nm shoulders are observed in curves 1–5 of Fig. 2(a) and curves 1–6 of Fig. 2(b); (3) 458 nm emitting is observed as main peak in curve 6 of Fig. 2(a) and shoulder in curve 7 of Fig. 2(a). Considering the broadest width of blue PL in Fig. 1(b) (than those in Fig. 2), it is reasonable that these fixed emitting points are also hidden in the blue emission of sample A, in which the observed redshift is a fraudulent feint due to the disappearance of short-wavelength components with increasing of excitation wavelength. Such below  $E_g$  excitation phenomena and stable emitting wavelengths have never been observed previously for the visible emissions of ZnO, and could provide some significant indications on the underlying defect origins.

The typical PLE spectrum is presented in Fig. 3, from which above remarkable excitation features show themselves again, exhibiting high accordance. First, the PLE peak at about 370 nm points out the similar optimal excitation wavelength to that in above ED-PL. Remarkably, there is a slowly dropping tail, which prolongs into violet region. This is just corresponding to above “below  $E_g$  excitation” phenomena. Such accordance is reflected by the similarity of excitation versus emission curve extracted from above ED-PL. Comparatively, the PLE spectrum of usual green emission exhibits a sharp drop, whose stopping wavelength is just  $E_g$ .

The fact that blue emissions can be effectively excited by  $E_{ex}<E_g$  energy demonstrates that the excited states and initial states of corresponding transitions could locate below the conduction band edge, not at or above conduction band edge. Under  $E_{ex}=E_g$  excitation, the electrons can be first excited up to conduction band, nonradiatively transit into above initial states, and then radiatively transit and emit blue emissions. The fixed emitting wavelengths indicate several different energy gaps from initial states to end states, such as 3.0 eV (412 nm), 2.8 eV (440 nm), and 2.7 eV (458 nm).

As to the detailed initial states, it can be analyzed from defect energy level and formation thermodynamics. Among

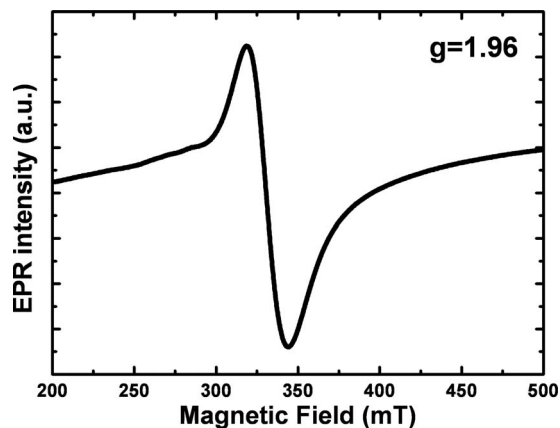


FIG. 4. EPR spectrum of ZnO hollow NPs with blue emissions.

the six types of point defects in ZnO lattice,  $V_{\text{O}}$ ,  $\text{Zn}_i$ , and  $\text{Zn}_\text{O}$  are donors, while  $V_{\text{Zn}}$ ,  $\text{O}_i$ , and  $\text{O}_{\text{Zn}}$  are acceptors. But, only  $\text{Zn}_i$  is the shallow donor<sup>15,16</sup> and the corresponding level could locate slightly below conduction band edge,<sup>15,17</sup> as revealed by many theoretical calculations and experimental results. Lin *et al.*<sup>18</sup> calculated the energy levels of various defect centers, and pointed out that the energy gap from the interstitial zinc level to the valence band is about 2.9 eV. Previously, Kroger and Bylander<sup>17,19</sup> experimentally determined that the Zn interstitial level is 0.22 eV below the conductive band edge. These reported level positions are very agreeable with the fixed violet shoulder at 412 nm (3.0 eV) in the blue emissions of this study. Look *et al.*<sup>15,16</sup> observed a shallow donor with ionization of 30 meV in ZnO crystal irradiated by high energy electrons, and assigned it to Zn interstitial or Zn interstitial-related complex defect. In the usual case, the formation energy of Zn interstitials is very high but it can be significantly reduced in Zn-rich environment,<sup>20,21</sup> which is just the important features for the formation process of ZnO NPs used in this study. Therefore, the observed initial state could be correlated with Zn interstitials, and there could be several derivative levels with lower energy, involving in possible localization or coupling with other defects. Finally, the highly nonequilibrium processes of LAL used for NP formation will greatly advance the formation of high concentration of Zn interstitials. Recently, Halliburton *et al.*<sup>22</sup> observed the increasing concentration of free carriers in the ZnO crystal annealed in Zn vapor. They attributed it to formed Zn interstitials and also suggested that the nonequilibrium conditions are beneficial to formation of Zn interstitials. Due to the possible energy difference of these derivative levels related to Zn interstitials, it is difficult to clearly identify the end states of transitions, which could locate at valence band or deep defect level slightly above valence band.

Such Zn interstitials assignment is further verified by the EPR measurements. For all the samples with strong blue emissions, a  $g=1.96$  factor is observed as shown in Fig. 4. This high-field signal was sometimes mistakenly attributed to unpaired electrons trapped on oxygen vacancies<sup>23</sup> and has

been identified to shallow donor centers.<sup>24</sup> Regardless of extrinsic impurities in ZnO, e.g., Al, Ga, In, it should be intrinsic Zn interstitials here.

In summary, strong blue luminescence was observed from ZnO hollow NPs, exhibiting well stability. Significantly, dramatic excitation dependence was observed for blue emissions: (1)  $E_{\text{ex}}=E_g$  energy is the optimal excitation but  $E_{\text{ex}}<E_g$  energy can still effectively excite blue emissions; (2) there exist several fixed emitting wavelengths in blue wave band, such as 412, 439, and 458 nm. Combined with previously reported defect levels and formation thermodynamics, these phenomena indicate that the initial states of corresponding transitions to blue emissions should be zinc interstitials-related defect states. Subsequent EPR examinations further verify this assignment.

This work was financially supported by NSFC (Grant Nos. 10604055 and 50831005), the National Basic Research Program of China (Grant No. 2007CB936604), and the Knowledge Innovation Program of the Chinese Academy of Sciences (Grant No. KJCX2-SW-W31).

<sup>1</sup>W. Park and G. Yi, *Adv. Mater.* **16**, 87 (2004).

<sup>2</sup>H. B. Zeng, X. J. Xu, Y. Bando, U. K. Gautam, T. Y. Zhai, X. S. Fang, B. D. Liu, and D. Golberg, *Adv. Funct. Mater.* **19**, 3165 (2009).

<sup>3</sup>M. H. Huang, S. Mao, H. Feick, H. Q. Yan, Y. Y. Wu, H. Kind, E. Weber, R. Russo, and P. D. Yang, *Science* **292**, 1897 (2001).

<sup>4</sup>U. K. Gautam, L. S. Panchakarla, B. Dierre, X. Fang, Y. Bando, T. Sekiguchi, A. Govindaraj, D. Golberg, and C. N. R. Rao, *Adv. Funct. Mater.* **19**, 131 (2009).

<sup>5</sup>Ü. Özgür, Y. Alivov, C. Liu, A. Teke, M. Reshchikov, S. Dogan, V. Avrutin, S. Cho, and H. Morkoc, *J. Appl. Phys.* **98**, 041301 (2005).

<sup>6</sup>L. Schmidt-Mende and J. L. MacManus-Driscoll, *Mater. Today* **10**, 40 (2007).

<sup>7</sup>Y. H. Yang, X. Y. Chen, Y. Feng, and G. W. Yang, *Nano Lett.* **7**, 3879 (2007).

<sup>8</sup>N. W. Wang, Y. H. Yang, and G. W. Yang, *J. Phys. Chem. C* **113**, 15480 (2009).

<sup>9</sup>F. H. Leiter, H. R. Alves, N. G. Romanov, D. M. Hofmann, and B. K. Meyer, *Physica B* **340**, 201 (2003).

<sup>10</sup>A. B. Djurišić and Y. H. Leung, *Small* **2**, 944 (2006).

<sup>11</sup>H. B. Zeng, W. P. Cai, J. L. Hu, G. T. Duan, P. S. Liu, and Y. Li, *Appl. Phys. Lett.* **88**, 171910 (2006).

<sup>12</sup>J. J. Wu and S. C. Liu, *Adv. Mater.* **14**, 215 (2002).

<sup>13</sup>H. B. Zeng, W. P. Cai, Y. Li, J. L. Hu, and P. S. Liu, *J. Phys. Chem. B* **109**, 18260 (2005).

<sup>14</sup>H. B. Zeng, W. P. Cai, P. S. Liu, X. X. Xu, H. J. Zhou, C. Klingshirn, H. Kalt, *ACS Nano* **2**, 1661 (2008).

<sup>15</sup>D. C. Look and J. W. Hemsky, *Phys. Rev. Lett.* **82**, 2552 (1999).

<sup>16</sup>D. C. Look, G. C. Falow, P. Reunchan, S. Limpijumnong, S. B. Zhang, and K. Nordlund, *Phys. Rev. Lett.* **95**, 225502 (2005).

<sup>17</sup>F. A. Kröger, *The Chemistry of Imperfect Crystals*, 2nd ed. (North Holland, Amsterdam, 1974).

<sup>18</sup>B. X. Lin, Z. X. Fu, and Y. B. Jia, *Appl. Phys. Lett.* **79**, 943 (2001).

<sup>19</sup>E. G. Bylander, *J. Appl. Phys.* **49**, 1188 (1978).

<sup>20</sup>P. Erhart, K. Albe, and A. Klein, *Phys. Rev. B* **73**, 205203 (2006).

<sup>21</sup>A. F. Kohan, G. Ceder, D. Morgan, and C. G. Van de Walle, *Phys. Rev. B* **61**, 15019 (2000).

<sup>22</sup>L. E. Halliburton, N. C. Giles, N. Y. Garces, M. Luo, C. C. Xu, L. H. Bai, and L. A. Boatner, *Appl. Phys. Lett.* **87**, 172108 (2005).

<sup>23</sup>K. Vanheusden, C. H. Seager, W. L. Warren, D. R. Tallant, and J. A. Voigt, *Appl. Phys. Lett.* **68**, 403 (1996).

<sup>24</sup>N. Y. Garces, L. Wang, L. Bai, N. C. Giles, L. E. Halliburton, and G. Cantwell, *Appl. Phys. Lett.* **81**, 622 (2002).